

## Supporting Information

# Harnessing Tunable Scanning Probe Techniques to Measure Shear Enhanced Adhesion of Gecko-Inspired Fibrillar Arrays

*Yasong Li<sup>1</sup>, James H.-W. Zhou<sup>3</sup>, Cheng Zhang<sup>2</sup>, Carlo Menon<sup>1</sup>, and Byron D. Gates<sup>3\*</sup>*

<sup>1</sup> Menrva Lab, School of Engineering Science, Simon Fraser University, 8888 University Drive, Burnaby, BC, V5A 1S6, Canada

<sup>2</sup> School of Engineering Science, Simon Fraser University, 8888 University Drive, Burnaby, BC, V5A 1S6, Canada

<sup>3</sup> Department of Chemistry and 4D LABS, Simon Fraser University, 8888 University Drive Burnaby, BC, V5A 1S6, Canada

\*E-mail: [bgates@sfu.ca](mailto:bgates@sfu.ca)

### Acknowledgements

This work was supported in part by the Natural Sciences and Engineering Research Council (NSERC) of Canada, and the Canada Research Chairs Program (B.D. Gates). This work made use of 4D LABS shared facilities supported by the Canada Foundation for Innovation (CFI), British Columbia Knowledge Development Fund (BCKDF), Western Economic Diversification Canada, and Simon Fraser University. We appreciate the assistance of Jason Bemis at Asylum Research for assistance in co-developing the software necessary for measuring adhesion forces resulting from shear induced alignment of fibrils using scanning probe microscopy techniques.

## **1. Experimental Section**

### **1.1. Fabrication of polymeric fibrillar dry adhesives**

The fibrillar arrays were fabricated using an epoxy-based photoresist (SU-8 2010, MicroChem) following a recipe detailed in previous work.<sup>1</sup> The polymer was patterned into 1 mm x 1 mm squares on a silicon wafer using photolithographic procedures, and etched in a Reactive Ion Etching (RIE) system (Etchlab 200, Sentech). The length of this etching process was proportional to the lengths of the resulting fibrils. The samples used in this study were prepared by etching for either 5 or 30 min with nominal fibril lengths of  $\sim 0.1$  and  $\sim 1$   $\mu\text{m}$ , respectively, as verified by scanning electron microscopy (Strata DB-235 SEM, FEI). Samples were also further inspected by SEM after the adhesion force measurements to investigate potential destruction of the surfaces. There was, however, no observable sample damage following the adhesion force measurements, which was consistent with the results of previous studies.<sup>2</sup> Prior to each measurement the samples were also examined for larger scale defects or contamination in the samples using an optical microscope (Axio Imager M1m, Zeiss).

### **1.2. Measurement of adhesion forces in fibrillar dry adhesives**

The adhesion force measurements were conducted using a scanning probe microscope (MFP-3D-SA AFM, Asylum Research) and a customized script written (with assistance from Jason Bemis, Asylum Research, Santa Barbara, CA) for specific motion control over the manipulations of the AFM probe. Tipless silicon nitride cantilevers (specifically the triangle labeled “C” in the NP-O10 probes, Veeco Instruments) were manipulated in order to approach, interact with and withdraw from the fibrillar surfaces with specific

control over different parameters. The cantilevers had a resonance frequency of  $\sim 60$  kHz within the range (40 – 75 kHz) provided in manufacturer's datasheet, and a spring constant of  $\sim 0.32$  N/m within the range (0.12 – 0.48 N/m) suggested by the manufacturer. These controlled parameters included the lateral and vertical position of the cantilever, lateral and vertical velocity of the cantilever and the interactive forces. To implement the LDP method for adhesion force measurements described in this study, the cantilever was controlled to follow a trajectory that largely represented a “sewing” type of motion. The cantilever was first brought into contact with the sample's surfaces in a vertical motion until reaching a preset force ( $\sim 55$  nN). At this preset position, the cantilever was moved in a lateral shear. Our study investigated a combination of different distances and velocities for this lateral shear before pulling the cantilever away from the surfaces in a vertical retraction. The retraction ended after a complete separation of the two surfaces. The cantilever was subsequently moved to another location on the sample to repeat the process for a second measurement, and this process repeated for a total of 400 measurements. The force exerted during the final vertical displacement, (i.e. the pull-off force) was measured as a single data point. Spring constant of the cantilever ( $\sim 0.32$  N/m) and resonance frequency ( $\sim 60$  kHz) were calibrated before acquiring each set of measurements, and were subsequently used in the adhesion force calculations. For each measurement cycle, a Force-Time (FT) curve was also recorded, which depicted the cantilever response curve with respect to the time elapsed during each cycle. In these measurements the FT curve for each cantilever-sample interaction can be interpreted using a simple beam model.

The three most important parameters for the subsequent set of LDP measurements were the lateral distance and velocity of the contacting surfaces during the applied lateral shear, and the velocity at which the two surfaces were separated. The ranges evaluated for each of these parameters was 0 – 2.5  $\mu\text{m}$ , 2 – 200  $\mu\text{m/s}$  and 0.1 – 4  $\mu\text{m/s}$ , respectively. The extremes in each set of experimental parameters were determined by the current limitations of our instrumentation. The default values for these parameters were set at a 1  $\mu\text{m}$  drag distance, a 20  $\mu\text{m/s}$  drag velocity and a 1  $\mu\text{m/s}$  retraction velocity. During the systematic investigation of one parameter, the other parameters were held constant, set at their default values; only one parameter was tuned at a time for each set of measurements. Each set of measurements consisted of 400 independent data points obtained from different locations on a sample. Further detail of the force measurements obtained using a SPM system using the LDP method can be found in our previous work.<sup>2</sup>

### **1.3. Statistical analysis of experimental results**

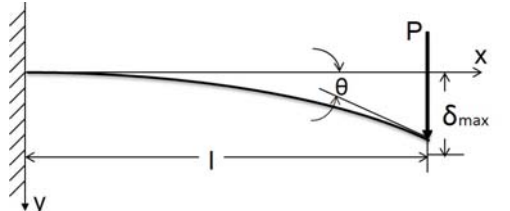
The statistical analysis used herein was performed, in part, using methods demonstrated in our previous studies.<sup>3</sup> Each analysis was performed on 400 data points for each type of measurement. Each data set was plotted as a histogram in order to visualize trends in the population. Two indicators of trends in the population, median and 12.5% trimmed mean, were calculated for each test parameter to help interpret the calculated average adhesion force. The median was calculated from the average of the two central most values for a sorted dataset of 400 individual points. The 12.5% trimmed mean was calculated from the average of 300 data points, which were selected from the original 400 data points by excluding equal portion of outliers from either side of the mean. Determination of the

percentage of trimmed data was based on a close examination of a normal probability plot. From observing the shape of the histograms plotted, we observed that the data did not follow a normal distribution. Therefore, without fulfilling the necessary assumptions, a traditional ANOVA analysis would be invalid for this study. A nonparametric test method, Kruskal-Wallis one-way ANOVA,<sup>3</sup> was used to indicate if the parameter of interest is significantly influencing the measured adhesion forces between the two surfaces. Levene's test <sup>3</sup> was used to compare the variances between different sets of measurements within each study.

## 2. Estimation of contact area in the adhesion force measurements

In this estimation the cantilever will be treated as a simple beam. The preloading force is treated as a point load acting on the end of the beam. The deformation model of this beam is provided by the equations in Table S1.<sup>4,5</sup>

**Table S1.** Equations related to cantilever deformation with respect to an applied load at the free end of a single beam.

schematic of the loading beam	slope at free end	deflection at any section in terms of x	maximum deflection
	$\theta = \frac{Pl^2}{2EI}$	$y = \frac{Px^2}{6EI} (3l - x)$	$\delta_{max} = \frac{Pl^3}{3EI}$

During each of the adhesion force measurements the deflection of the free end of the cantilever (i.e. maximum deflection  $\delta_{max}$  indicated in Table S1) upon reaching the initial preload force (upon initial contact between the cantilever and the sample) was determined

to be  $\sim 127$  nm from the inverse optical lever sensitivity or InvOLS. This InvOLS value was derived using the scanning probe microscope software controlling the cantilever. Length of the beam ( $l$ ) was  $120 \mu\text{m}$  as per the nominal cantilever length reported on the manufacturer's datasheet, and the preload force was  $\sim 55$  nN as determined from the calibration of the cantilever spring constant. Therefore:

The maximum deflection is:

$$\delta_{max} = \frac{Pl^2}{2EI} \frac{l}{3} = \frac{2\theta l}{3}$$

And the slope at the free end of the beam due to this deflection is:

$$\theta = \frac{3\delta_{max}}{2l} = \frac{0.127 \times 3}{120 \times 2} = 0.0015875 = 0.09^\circ$$

This value is very small in comparison to the angle between the cantilever plane and the sample plane, which is  $11^\circ$ . Therefore, the contribution from the maximum deflection of the cantilever was negligible when determining the contact area.

Figure S1 depicts a side-view for the geometry of a cantilever upon contact with the fibrillar sample.

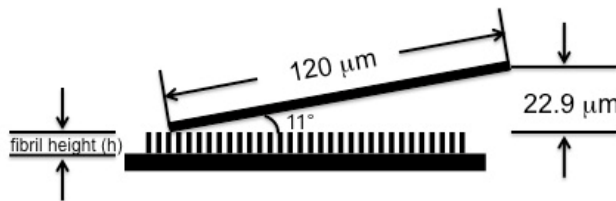


**Figure S1.** Schematic depiction showing the side-view for the interactions of a cantilever in contact with a fibrillar sample.

The distance between the free ends of the fibrils and the base of the cantilever, as determined by the fixed position of the cantilever base within the cantilever holder, was  $22.9 \mu\text{m}$ . In contrast to the free air deflection of the cantilever ( $127$  nm) and the distance

traveled by the cantilever base ( $1\ \mu\text{m}$ ), the separation from the base is significantly large. This separation and the angle of the approaching cantilever dictate a small (few micrometers in size) interaction area between the free end of cantilever and the fibrillar surfaces. The contact length ( $L$ , the length of cantilever in contact with the fibrils) is illustrated in Figure S2, and the magnitude of  $L$  is estimated as follows:

$$L = \frac{(h + \delta_{max})}{\tan 11^\circ}$$

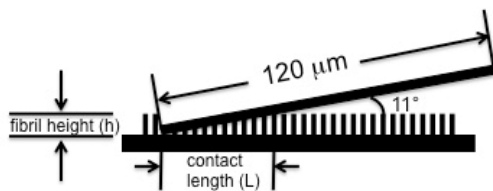


**Figure S2.** Schematic depiction of the contact length ( $L$ ) between the end of the cantilever and the fibrillar surfaces after reaching the preload set-point force.

For shorter fibrils ( $\sim 0.1\ \mu\text{m}$ ), the contact length was estimated to be:

$$L = (0.1 + 0.127) / \tan 11^\circ = 1.17\ \mu\text{m}$$

For longer fibrils ( $\sim 1\ \mu\text{m}$ ), the contact length was estimated to be:

$$L = (1 + 0.127) / \tan 11^\circ = 5.80\ \mu\text{m}$$

To determine the contact area from these estimated contact lengths, the top view of the cantilever geometry was measured by optical microscopy as depicted in Figure S3.

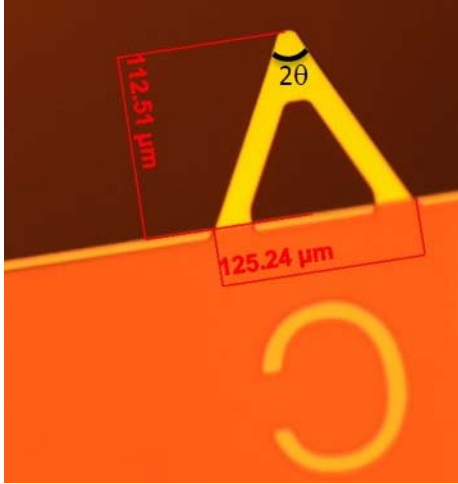


**Figure S3.** Optical microscope image showing the top view of the cantilever used in the adhesion force measurements.

Based on the geometry of the free end of the tipless cantilever, only the solid portions of the triangular area contributed to the potential contact area with the fibrillar sample. The angle at the end of this triangle corresponded to  $2\theta$  as indicated in Figure S3, and was derived from its relationship to the overall length of the cantilever and the width of its base (forming the sides of a triangle) as described by:

$$\tan\theta = \frac{125.24/2}{112.51} = 0.557$$

Therefore, the final contact area is estimated as follows.

For shorter fibrils, the contact area was estimated to be:

$$A = L \times L \tan\theta = 1.17 \times 1.17 \times 0.557 = 0.762 \mu\text{m}^2$$

For longer fibrils, the contact area was estimated to be:

$$A = L \times L \tan\theta = 5.8 \times 5.8 \times 0.557 = 18.7 \mu\text{m}^2$$

## References

- [1] Sameoto, D.; Li, Y.; Menon, C. Micromask Generation for Polymer Morphology Control: Nanohair Fabrication for Synthetic Dry Adhesives. *Adv. Sci. Tech.* **2008**, *54*, 439-444.
- [2] Li, Y.; Zhang, C.; Zhou, J. H.-W.; Menon, C.; Gates, B. D. Measuring Shear Induced Adhesion of Gecko-Inspired Fibrillar Arrays Using Scanning Probe Techniques. *Macromol. React. Eng.* **2013**, *7*, 638-645.
- [3] Montgomery, D. C. *Design and Analysis of Experiments*, 8th ed.; Wiley: Hoboken, NJ, **2013**.
- [4] Raj, P.P. & Ramasamy, V. *Strength of materials*, Dorling Kindersley, New Delhi, **2012**.
- [5] Beam Deflection formulae, Available from [http://www.advancepipeliner.com/Resources/Others/Beams/Beam\\_Deflection\\_Formulae.pdf](http://www.advancepipeliner.com/Resources/Others/Beams/Beam_Deflection_Formulae.pdf) [Accessed December 1, 2014].